

Strong contributions from surface electromagnetic fields to angle-resolved photoemission intensities of copper

F. Pforte, T. Michalke, A. Gerlach,* and A. Goldmann†

Fachbereich Physik, Universität Kassel, Heinrich-Plett-Strasse 40, D-34132 Kassel, Germany

R. Matzdorf‡

Physikalisches Institut, Universität Würzburg, Am Hubland, D-97074 Würzburg, Germany

(Received 18 May 2000; revised manuscript received 9 October 2000; published 26 February 2001)

Unexpected high photoemission intensity is observed on copper surfaces at grazing incidence angles of p -polarized light ($\hbar\omega = 21.2$ eV). The dipole approximation in combination with Fresnel's equations and the optical constants of copper is not sufficient to explain the experimental data. Instead, local electric-field effects at the surface have to be taken into account. In order to model the observed dependence of intensity on light incidence angle, we follow two different approaches: one using modified optical constants at the surface, and one including surface photoemission. Within both formulations excellent fits to our experimental intensities can be obtained, however, with the present data we cannot decide which model is more appropriate.

DOI: 10.1103/PhysRevB.63.115405

PACS number(s): 79.60.-i, 42.25.Bs, 73.20.-r

I. INTRODUCTION

The contribution of surface-related electromagnetic fields to photoelectron peak intensities has been discussed since the early days of photoemission experiments; see Feibelman's excellent review¹ for references to earlier work. Photoelectron spectroscopy^{2,3} is an extremely surface-sensitive technique due to electron escape depths of only a few lattice constants. When the electromagnetic field, required to excite photoelectrons, crosses the surface of a solid, the components of the electric field parallel to the surface vary continuously on a scale defined by the wavelength of the incident light. In contrast the normal component varies rapidly over distances of the order of Angstroms showing Friedel-like oscillations near the surface,¹ because the translational symmetry in this direction is broken. In classical terms this response is an induced surface charge,¹ quantum mechanically the response is the near-surface excitation of electron-hole pairs or plasmons.¹ Therefore any analysis of photoemission matrix elements cannot ignore this short-range dielectric response. The fundamental problem is, however, that not much is known about the local optical properties at the surface, and theoretical progress in calculating the screening at a surface has been limited to free-electron-like metal surfaces.¹ This theory refers to the surface of a jellium metal with the charge density of aluminum. It has been verified for photoemission intensities measured near the Fermi edge from Al(100), which shows a rapid resonance-like variation with photon energies in the energy range of the surface and bulk plasmons.⁴⁻⁶ The question related with our present paper is different: Can we identify experimentally any intensity contributions from surface-related fields to angle-resolved photoemission peaks measured at fixed photon energy $\hbar\omega = 21.2$ eV?

In time-dependent perturbation theory the transition rate w of photoemission is described as⁶

$$w \propto |M_{fi}|^2 \delta(E_f - E_i - \hbar\omega) \rho(E_f) \quad (1)$$

with initial- and final-state energies E_i and E_f , the photon energy $\hbar\omega$, the density of final states $\rho(E_f)$, and the matrix element

$$M_{fi} \propto \langle f | \mathbf{A} \cdot \mathbf{p} | i \rangle + \frac{\hbar}{2i} \langle f | \text{div} \mathbf{A} | i \rangle. \quad (2)$$

In this equation $\mathbf{A}(\mathbf{r})$ is the corresponding vector potential transmitted into the sample and \mathbf{p} is the momentum operator. In most textbooks on photoelectron spectroscopy the first term is identified with momentum conserving "direct transitions," while the second term is described as "surface emission" or emission induced by "local-field effects." In the majority of photoemission experiments analyzed in the past^{2,3,6} the second term in Eq. (2) has been simply neglected.^{7,8} The calculation of the transmitted vector potential \mathbf{A}^t from the incident field \mathbf{A}^i is based on the Maxwell theory. If the dielectric constant is assumed to change abruptly from $\varepsilon = 1$ in vacuum to $\varepsilon = \varepsilon_1 + i\varepsilon_2$ inside the sample, the amplitude of \mathbf{A}^t is spatially constant and follows from Fresnel's equations:⁹

$$A_x^t = \frac{2 \cos \psi}{\cos \psi + \sqrt{\varepsilon - \sin^2 \psi}} |\mathbf{A}^i|, \quad (3)$$

$$A_y^t = \frac{2 \cos \psi \sqrt{\varepsilon - \sin^2 \psi}}{\varepsilon \cos \psi + \sqrt{\varepsilon - \sin^2 \psi}} |\mathbf{A}^i|, \quad (4)$$

$$A_z^t = \frac{2 \cos \psi \sin \psi}{\varepsilon \cos \psi + \sqrt{\varepsilon - \sin^2 \psi}} |\mathbf{A}^i|, \quad (5)$$

where ψ is the light incidence angle within the optical plane (yz -plane). In this description both the incident and transmitted fields are transverse, with the consequence that $\text{div} \mathbf{A} = 0$, except just at the interface, as can be easily checked. In fact previous photoemission studies¹⁰⁻¹³ have shown that calculating \mathbf{A}^t with Fresnel's equations and the dielectric function of the bulk gives a fair overall description of the

experimental observations. However, our recent experiments with an improved experimental setup indicate that good fits to the experimental data either require modified dielectric constants (Sec. III A) or the inclusion of the second term in Eq. (2) into the analysis (Sec. III B). We discuss some representative data together with the subsequent analysis based on Eq. (2). Particularly we present evidence that the second term in Eq. (2), which results exclusively from local-field effects within the surface layers, may contribute significantly to the intensity of angle-resolved photoelectron peaks of bulk states as well as of surface states on copper.

II. EXPERIMENTAL DETAILS

Our spectrometer arrangement includes a high-resolution energy analyzer, a rotatable polarizer arrangement allowing to vary the incidence angle ψ of 93% p -polarized light at constant electron take-off angle θ , and the standard facilities for sample cleaning. Both light incidence and electron emission directions are confined to the same optical plane. In particular we mention that the geometry is optimized to collect all photoelectrons even at $\psi=80^\circ$. For details we refer to Ref. 14. The resolution parameters of the analyzer may be changed *in situ*. The energy resolution can be tuned down to $\Delta E=10$ meV. Also the angular resolution can be varied between $\Delta\theta=\pm 0.4^\circ$ and $\pm 1.5^\circ$. The samples (oriented to $\pm 0.3^\circ$) have been polished mechanically and electrochemically, cleaned *in situ* by argon ion bombardment and subsequently annealed. Sample cleanliness and surface order were verified by regular checks of the well-known^{2,3} surface states occurring on Cu(111) at the $\bar{\Gamma}$ point ($E_i=-0.39$ eV) and on Cu(110) at the \bar{Y} point ($E_i=-0.43$ eV) of the corresponding surface Brillouin zones.

III. RESULTS

A. Analysis without surface emission

In this section we present a concept to analyze photoemission intensities neglecting any spatial variation of surface related fields. Combining Eq. (2) with Fresnel's equations yields

$$M_{fi} \propto \mathbf{A}^t \cdot \langle f | \mathbf{p} | i \rangle = \mathbf{A}^t \cdot \mathbf{P}_{fi} \quad (6)$$

with the momentum matrix element \mathbf{P}_{fi} . This is the usual dipole approximation. In the Cartesian coordinates the transition matrix element is then given by

$$M_{fi} \propto A_x^t P_x^* + A_y^t P_y^* + A_z^t P_z^* \quad (7)$$

with the conjugate complex components P^* of \mathbf{P}_{fi} . For a certain transition, the complex vector \mathbf{P}_{fi} is a quantity that is independent of the vector potential and that is characteristic for the wave functions of the participating states. Its components are fixed with respect to the crystal lattice directions. In contrast the complex components of \mathbf{A}^t depend sensitively on \mathbf{A}^i and can therefore be tuned by variation of polarization and light incidence angle. In general the direction of \mathbf{P}_{fi} is not known *a priori*, but in this paper we have chosen some transitions, whose \mathbf{P}_{fi} can be derived from the symmetry of

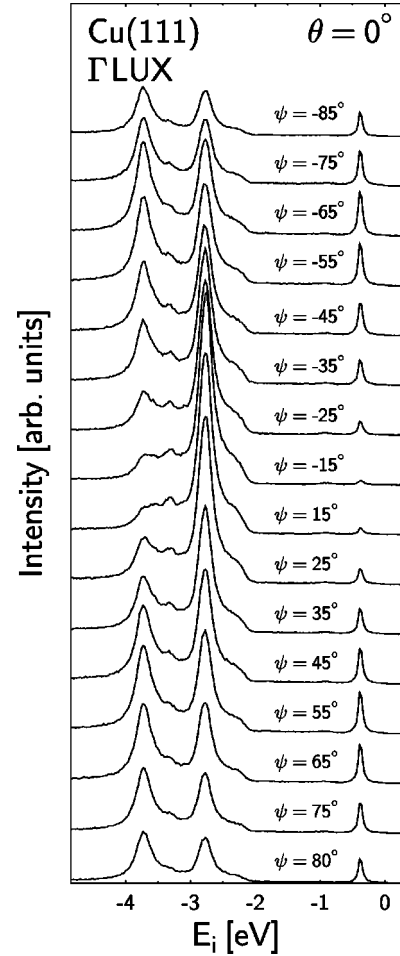


FIG. 1. Normal emission spectra excited with p -polarized He I radiation ($\hbar\omega=21.2$ eV) taken at different light incidence angles ψ . All data are normalized to equal incident photon flux.

the initial state. Thus we are able to probe experimentally to which extent \mathbf{A}^t can be described by Fresnel's equations (3)–(5).

Particularly we study the intensity dependence $I(\psi) \propto |M_{fi}|^2$ of well-defined emission peaks with p -polarized light, i.e., $A_x=0$. A typical experimental result is reproduced in Fig. 1 showing normal emission spectra from Cu(111) for light incidence along the Γ LUX mirror plane. All amplitudes are normalized to the same incident photon flux. The surface state at the $\bar{\Gamma}$ point ($E_i=-0.39$ eV) shows a symmetric intensity dependence $I(\psi) \approx I(-\psi)$: The intensities can be easily evaluated and are plotted in Fig. 2. The orbital character of the initial state is sp_z -like^{2,3} and therefore \mathbf{P}_{fi} is oriented along the surface normal. In consequence it can only be excited by the z component of \mathbf{A}^t , which gets zero at $\psi=0$. At grazing incidence the light is reflected totally, no photons can be adsorbed and the photoemission intensity vanishes.

Now we fit the square of Eq. (7) to the data points. Despite the known symmetry of the surface state we regarded the complex components P_y and P_z as free parameters in this analysis. Since only $|M_{fi}|^2$ is observable, the phase of the matrix element is undefined and we are free to choose P_z as

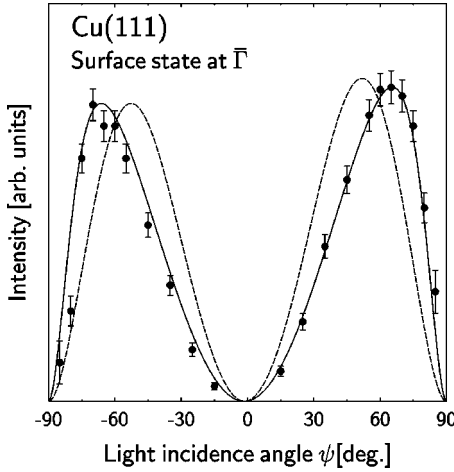


FIG. 2. Intensity $I(\psi)$ of the surface state observed at the $\bar{\Gamma}$ point ($E_i = -0.39$ eV) in Fig. 1 excited with p -polarized radiation as a function of the light incidence angle ψ . The curves through the data points are discussed in the text.

real. Therefore \mathbf{P}_{fi} can be expressed by a phase angle γ representing a phase shift between P_z and P_y and the angle β representing the direction of \mathbf{P}_{fi} with respect to the sample normal:

$$P_y = |\mathbf{P}_{fi}| \sin \beta e^{i\gamma}, \quad (8)$$

$$P_z = |\mathbf{P}_{fi}| \cos \beta. \quad (9)$$

Using Fresnel's equations (4) and (5) for A_y^t and A_z^t and the well-known bulk dielectric constant $\epsilon_b = 0.63 + i0.74$ of Cu at 21.2 eV,^{15,16} we obtain the dashed curve shown in Fig. 2. This fit results in $\beta = (1.5 \pm 3.0)^\circ$, which is in good agreement with $P_y = 0$ as expected. Thus we essentially measure the angular dependence of $A_z^t(\psi)$, because $I \propto |A_z^t(\psi)|^2$ in this case. Since the intensity distribution $I(\psi)$ is completely determined by the dielectric constant entering Fresnel's equation, we have to change ϵ in order to improve the fit. This results in $\epsilon_s = 1.03 + i0.22$ (solid line in Fig. 2), which is clearly off the bulk dielectric constant: Typical error bars (of this and further results discussed below) are $\epsilon_s = (\epsilon_1 \pm 0.10) + i(\epsilon_2 \pm 0.10)$. Variation of ϵ_s within its error bars is still consistent with the aforementioned value of β .

As a second example on Cu(111) we have studied the photoemission peak at $E_i = -3.70$ eV in Fig. 1, which shows a similar intensity dependence as the surface state. A detailed analysis, also checking for differently defined background subtractions, results in $\beta = (-1.1 \pm 3.0)^\circ$ if we use ϵ_b .¹⁷ Again this fit (not shown here) cannot describe the measured intensities. Much better agreement is obtained with ϵ_s as given above. In the latter case we calculate $\beta = (1.4 \pm 3.0)^\circ$ in perfect agreement with the value obtained with ϵ_b . It is our general experience with many data sets at different θ and E_i that the direction of \mathbf{P}_{fi} does not depend sensitively on the particular choice of ϵ . In all cases investigated at Cu(110) and Cu(111) surfaces we observe that $\epsilon_s \neq \epsilon_b$.

Furthermore we have studied photoemission intensities from Cu(110) at $\hbar\omega = 21.2$ eV and with θ and ψ confined to

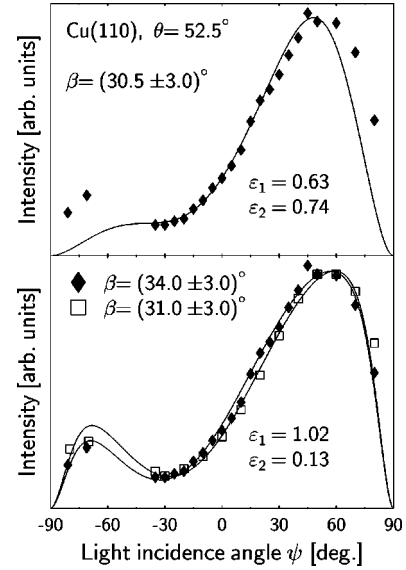


FIG. 3. Photoemission intensities $I(\psi)$ obtained from Cu(110) at $\theta = 52.5^\circ$ ($E_i = -3.70$ eV) in the Γ LUX plane vs incidence angle ψ . The electric field with $\hbar\omega = 21.2$ eV was p -polarized with respect to this mirror plane. Top: fit of Eq. (7) with ϵ_1, ϵ_2 as indicated. Bottom: same data as top (filled diamonds) fitted with $\epsilon_s = 1.02 + i0.13$. Open squares show data points from a different experiment with the same values for ϵ_s .

the Γ LUX bulk mirror plane. Under appropriate kinematical conditions direct emission with $E_i = -3.70$ eV occurs just at the same k space point along the Γ L direction as in case of normal emission from Cu(111). Indeed experimental peak positions observed from Cu(110) are almost the same as from Cu(111), and for this particular energy they have been made identical ("energy coincidence method," see Refs. 2 and 3). Since the matrix element only depends on the wave functions of the participating states in the bulk, the direction of \mathbf{P}_{fi} must not depend on the particular surface orientation. From the Cu(111) normal emission results we already know that \mathbf{P}_{fi} is parallel to the Γ L direction. According to the geometry of the Γ LUX plane we expect $\beta = 35.3^\circ$ on Cu(110). The measured intensities from Cu(110) at $E_i = -3.70$ eV and $\theta = 52.5^\circ$ are reproduced in Fig. 3, top panel. A fit with Eq. (7) using ϵ_b results in the solid line, which does not describe the measured intensities adequately at large light incidence angles. Again a more convincing fit is achieved with a different dielectric constant, see the lower panel of Fig. 3. The bottom panel also shows a set of results obtained with a different sample (open squares) demonstrating the typical reproducibility. Figure 3 shows three fits giving results for β . As an average from the lower panel we take $\beta = (33 \pm 3)^\circ$, in perfect agreement with the expected value. Thus we only need to vary ϵ_1 and ϵ_2 , i.e., the parameters describing the dielectric response, in a fit of Eq. (7) with $A_x = 0$. Our result from several fits is $\epsilon_s = (1.02 \pm 0.10) + i(0.20 \pm 0.10)$, which is definitely far off the bulk value.

One may ask why this discrepancy was not resolved in earlier studies of our group^{12,13} and other authors.^{10,11} This can be traced back to some improvements of our experimental arrangement. In the earlier studies^{12,13} the rotatable polar-

izer could be turned between 30° and 180° with respect to the electron lens axis. For the remaining light incidence angles the sample had to be rotated azimuthally. Therefore the range of accessible light incidence angles contained an interval of 60° where no data could be taken. This made all fits much less reliable compared to the present measurements. Furthermore and even more important, we improved our lens system in front of the energy analyzer. First, the distance between sample and lens entrance was increased and the polarizer can now be rotated by 360° around the manipulator axis. Second the blocked interval could be reduced to 30° in total. Third, the transfer lens now accepts electrons from a larger light spot on the sample surface. In consequence practically *all* photoelectrons are collected for $\psi \leq 80^\circ$, contrary to the earlier arrangements.¹⁰⁻¹³ Indeed the new experimental data show clear intensity enhancement at large light incidence angles compared to the old data. An earlier study¹⁰ of Cu(110) at $\theta = 52^\circ$ ($\hbar\omega = 21.2$ eV), which could vary ψ between zero and $+76^\circ$ had already detected deviations of $I(\psi)$ taken for $\psi > 0$. From the best fit of Fresnel's equations these authors derived the numbers $\varepsilon_1 = 0.89$ and $\varepsilon_2 = 0.48$, which are intermediate between ε_b and our results of ε_s . The authors, however, concluded that their modified optical constants "deviate appreciably from the known values" and therefore believed them to be insignificant.¹⁰

Figure 4 shows the consequence of the different dielectric constants on the components of the transmitted vector field \mathbf{A}^t assuming that ε is isotropic. With respect to A_z^t , the real part is enhanced drastically at $\psi > 60^\circ$ by ε_s (solid line), while the imaginary component is reduced at $\psi < 70^\circ$ compared to the calculated bulk field (dotted line). Also the imaginary part of A_y^t gets smaller using ε_s especially at $\psi < 45^\circ$, but this effect is obviously less dramatic than with A_z^t . The calculation reproduced in Fig. 4 also predicts significant changes in A_x , which cannot be checked with our present experimental arrangement. The increased z component at large light incidence angles and the only small modification of the y component by ε_s indicates a dominant surface related change of the electromagnetic field. Such behavior is consistent with a contribution of the second term appearing in Eq. (2). Therefore we have tried to model this term using plausible assumptions and to include it into our analysis. This will be the subject of Sec. III B.

B. Analysis including surface emission

No general method to calculate the second term in Eq. (2) is available. In order to develop an at least reasonable approximation for the integral containing $\text{div } \mathbf{A}$, we exploit the symmetry at the surface. On the scale of Angstroms the field polarized parallel to the surface is spatially a constant. Therefore no surface charge can be induced and any microscopic effect can be safely ignored. The incident long-wavelength field, however, may induce a short-wavelength response if the electric field contains components polarized perpendicular to the surface. In consequence exclusively the z component of \mathbf{A} may contribute to the surface photoeffect.

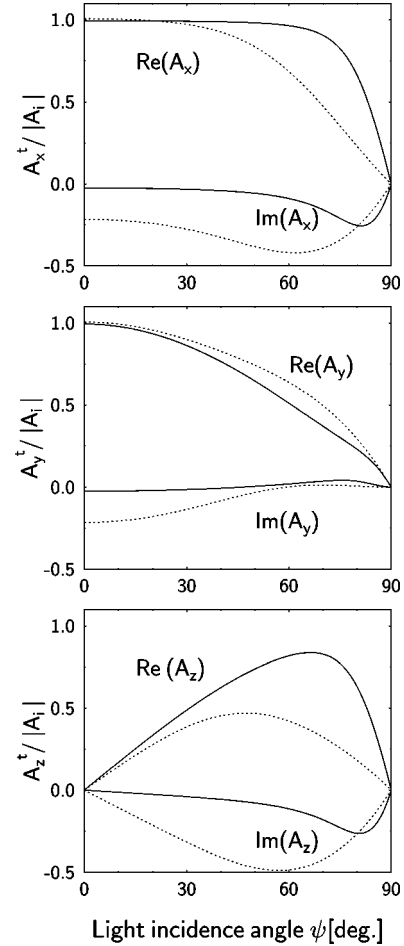


FIG. 4. Calculated Cartesian components of the transmitted vector potential \mathbf{A}^t related to the incident field \mathbf{A}^i and the light incidence angle ψ . The two curves represent real part (Re) and imaginary part (Im). All curves are calculated with Fresnel's equations and $\varepsilon_b = 0.63 + i0.74$ (dotted lines) or $\varepsilon_s = 1.02 + i0.10$ (solid lines).

We assume that the electron system needs a layer of thickness d for screening and that the vector potential varies from \mathbf{A}^i to \mathbf{A}^t on this length according to

$$\mathbf{A}(\mathbf{r}, t) = \mathbf{A}^0(z) \exp(i\mathbf{k}_p \cdot \mathbf{r} - i\omega t), \quad (10)$$

where \mathbf{k}_p is the photon wave vector and Eq. (10) represents \mathbf{A} entering the second term of Eq. (2). Calculating $\text{div } \mathbf{A}$ yields

$$\text{div } \mathbf{A} = \mathbf{A}^0 \cdot i\mathbf{k}_p \exp(i\mathbf{k}_p \cdot \mathbf{r} - i\omega t) + \frac{\partial A_z^0}{\partial z} \exp(i\mathbf{k}_p \cdot \mathbf{r} - i\omega t). \quad (11)$$

In Coulomb gauge the first term is zero everywhere, because the wave is transversal. Due to the translational symmetry within the plane of the surface, momentum conservation in these directions still applies to the matrix element $\langle f | \text{div } \mathbf{A} | i \rangle$ and we get

$$E_f = E_i + \hbar\omega \quad \text{and} \quad \mathbf{k}_f^\parallel = \mathbf{k}_i^\parallel + \mathbf{k}_p^\parallel \quad (12)$$

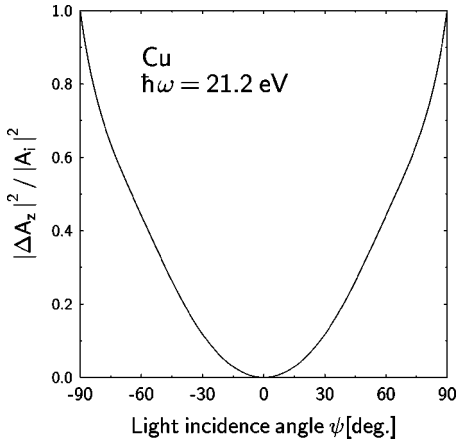


FIG. 5. Angular dependence of $\text{div } \mathbf{A}$ within the linear approximation according to Eq. (14) using the bulk optical constants of Cu at $\hbar\omega = 21.2$ eV. We have plotted $|\Delta A_z|^2 \propto |\partial A_z^0 / \partial z|^2$. The contribution of surface emission increases with the light incidence angle ψ and can be neglected at $\psi = 0$.

with E the electron energies and \mathbf{k}^\parallel the wave vectors parallel to the surface of the initial state, final state, and photon, respectively. Therefore the measured intensities are \mathbf{k}^\parallel resolved, regardless if $\text{div } \mathbf{A}$ enters the complete matrix element.

While the surface preserves momentum in two directions, the conservation in the z direction is broken. Here both terms appearing in Eq. (2) have to be considered separately. Conservation of k_\perp in direct transitions requires the contribution of a reciprocal lattice vector, because the momentum of the photon is almost negligible compared to the momentum change in the photoemission process.^{2,3} In case of surface emission the rapid variation in the normal component of the electric field acts as a source of momentum via the uncertainty principle, enabling an electron to absorb a photon. In a direct transition some uncertainty of k_\perp is introduced via the lifetime of the final state,⁶ and it is given by $2\pi/l$ with a mean-free-path l of the excited electron. For surface emission the additional uncertainty is due to $\text{div } \mathbf{A}$, which is non-zero only in the surface layer of width d . The resulting uncertainty is then given by $2\pi/d$.

The consequences for surface photoemission are evident. If d is comparable with the lattice constant a the uncertainty of k_\perp is given by the size of the Brillouin zone. In the general case $a < d < l$ one must consider carefully that the widths of direct emission features induced by the first or the second term in Eq. (2) may be actually different. As also seen from Eq. (2) the amplitudes of direct and surface emission may interfere. If there is a rapid change of relative phases across the width of the direct emission peak, also the peak shape may be drastically affected.^{7,8} However, no dependence on k_\perp is relevant for photoemission from two-dimensional (2D) surface bands. In this case the same peak shape can be expected for contributions from the direct and surface emission intensities, respectively.

For further data analysis we must model the second term in Eq. (11). Following Ref. 7 we introduce a linear approximation

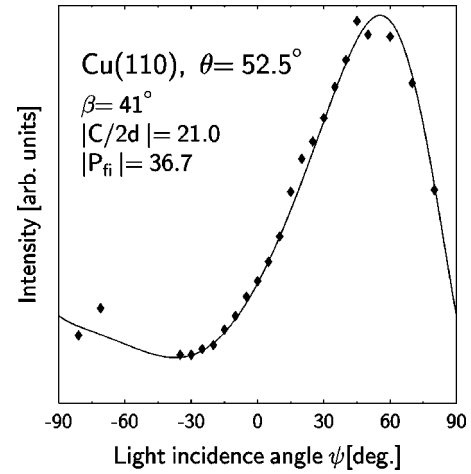


FIG. 6. Experimental intensities taken from Fig. 3. The solid lines represent a fit according to the square of Eq. (15), using the bulk optical constants ϵ_b of Cu at $\hbar\omega = 21.2$ eV. Due to the inclusion of surface emission the enhanced intensities at larger light incidence angles are reproduced.

$$\frac{\partial A_z^0}{\partial z} \approx \frac{A_z^t - A_z^i}{d} = \frac{\Delta A_z}{d}. \quad (13)$$

The field component A_z^t is expressed via Fresnel's equation, whereas the incident light is simply $A_z^i = |\mathbf{A}^i| \sin \psi$. Combining this with Eqs. (5) and (13) results in

$$\frac{\Delta A_z}{d} = \frac{|\mathbf{A}^i|}{d} \left(\frac{2 \cos \psi \sin \psi}{\epsilon \cos \psi + \sqrt{\epsilon - \sin^2 \psi}} - \sin \psi \right). \quad (14)$$

The angular dependence of $|\Delta A_z|^2$ is shown in Fig. 5. As expected we get $\Delta A_z = 0$ at $\psi = 0$. Remarkably, it reaches its maximum amplitude at $\psi = 90^\circ$. The reason is that at grazing incidence no light is transmitted into the sample, and the jump between A_z^t and A_z^i attains its maximum. Such a behavior seems to be compatible with our data reproduced in Figs. 2 and 3: The strongest deviation of the experimental intensities from the fit using bulk optical constants occurs at large ψ values. In contrast, good agreement was found around $\psi = 0$.

Collecting everything we may express Eq. (2) as

$$M_{fi} \propto \mathbf{A}^t \cdot \mathbf{P}_{fi} + \frac{\Delta A_z}{d} \frac{C}{2}, \quad (15)$$

where we have combined all unknown factors in the complex number $C/2$. A fit of $|M_{fi}|^2$, now treating the first term in Eq. (2) as before with the use of Fresnel's equations but using the bulk optical constants $\epsilon_1 = 0.63$ and $\epsilon_2 = 0.74$, is shown in Fig. 6 for the data set shown already in Fig. 3. As is obvious the agreement with Eq. (15) is excellent. Similarly we may use Eq. (15) to fit the $I(\psi)$ points treated before in Fig. 2. The result is reproduced in Fig. 7, which shows two fits using exclusively the bulk dielectric function: The solid line includes the second term shown in Eq. (15), while the

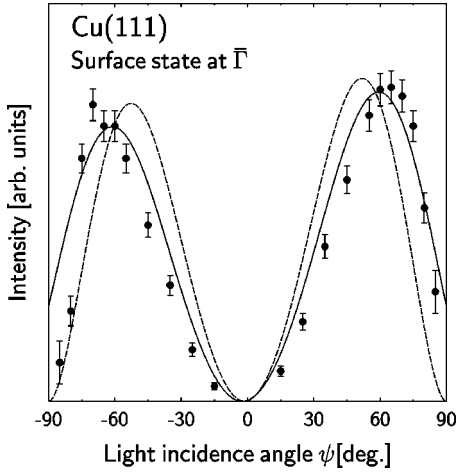


FIG. 7. Experimental intensities taken from Fig. 2. The dashed line shows the intensity variation with $\epsilon_b = 0.63 + i0.74$ whereas the solid line represents a fit with surface emission using the same values for ϵ_0 .

dashed line is calculated with the second term (surface emission) neglected. Again, consideration of the $\text{div } \mathbf{A}$ term improves the fit considerably.

With regard to the various fit parameters, it is interesting to compare the results obtained with either bulk or surface-modified optical constants. In all cases the angle β , which indicates the orientation of \mathbf{P}_{fi} within the light incidence plane, is essentially unchanged within the error bars. This is an important result. It indicates that earlier studies that determined the direction of \mathbf{P}_{fi} exclusively from the assumption that $M_{fi} \propto \mathbf{A}^t \cdot \mathbf{P}_{fi}$, i.e., with surface emission neglected, are basically correct with respect to β . The reason is obvious: First, β is dominated by the symmetry (or asymmetry) around $\psi = 0$, whereas the surface term enters $I(\psi)$ only at the largest angles of incidence. Second, the fit parameters $|C/2d|$ are of the same order of magnitude as $|\mathbf{P}_{fi}|$. This means that at intermediate angles between 0 and 90° both the direct-transition term and the surface-emission term contribute almost equally to the experimental intensity $I(\psi)$, whereas the intensity for $\psi \rightarrow \pm 90^\circ$ results exclusively from the matrix element containing $\text{div } \mathbf{A}$.

IV. DISCUSSION AND SUMMARY

We have collected photoelectron spectra at various incidence angles ψ of p -polarized light with all other kinematical parameters fixed. The intensity distributions $I(\psi)$ cannot be described satisfactorily using the “standard” matrix element in dipole approximation

$$I(\psi) \propto |\langle f | \mathbf{A} \cdot \mathbf{p} | i \rangle|^2 = |\mathbf{A} \cdot \mathbf{P}_{fi}|^2$$

if the transmitted vector potential \mathbf{A} is calculated on the basis of bulk optical constants and Fresnel’s equations. There are two possible refinements that result in much better agreement with experiment.

First, the $I(\psi)$ dependence is in accord with Eq. (7) and with \mathbf{A}^t calculated by Fresnel’s equation, if and only if, we use empirical surface dielectric constants ϵ_s which differ

considerably from the bulk value ϵ_b . Analyzing transitions of bulk and surface states on Cu(111) and Cu(110) with a photon energy of $\hbar\omega = 21.2$ eV, the modified surface dielectric constant was found to be $\epsilon_s = (1.0 \pm 0.1) + i(0.1 \pm 0.1)$. This is clearly different from the bulk value $\epsilon_b = 0.63 + i0.74$. The ordinary theory of refraction, i.e., Fresnel’s equations combined with ϵ_1, ϵ_2 , treats copper as an optically homogeneous medium and averages over scales given by the light wavelength ($\lambda = 580$ Å at 21.2 eV) and/or the mean-free-path of the photons $t = \lambda / (4\pi k)$ ($t = 120$ Å at 21.2 eV) where k is the absorption constant of copper.²¹ In contrast the electron mean-free-path relevant for our photoemission results is approximately 10 Å^{2,3} and we cannot expect to measure the optical constants of the bulk in photoemission experiments. Within a microscopic description of the dielectric response at the surface ϵ is treated as a tensor. Therefore the high photoemission intensity at large light incidence angles may indicate the anisotropic dielectric response in the outermost layers of the solid. This is supported by experimental evidence from reflectance anisotropy spectroscopy (RAS) from Cu(110) at $\hbar\omega = 1.4$ – 4.0 eV: The amplitude for surface reflection of light incident normally and polarized linearly is anisotropic with respect to the bulk crystal directions [001] and $[\bar{1}10]$, see e.g., Refs. 18–20. This is a clear indication that even in this case the surface optics cannot be described properly by isotropic optical constants. Especially in the direction perpendicular to the surface there should be severe modifications of the optical constants.

Second, we used Fresnel’s equations in combination with ϵ_b to calculate $|\mathbf{A} \cdot \mathbf{P}_{fi}|^2$, but included the matrix element $\langle f | \text{div } \mathbf{A} | i \rangle$ responsible for surface emission in the data analysis. Again an almost perfect agreement with experiment could be obtained. This approach is problematic, too in that no microscopic theory is available to calculate the surface electric field component A_z . Therefore $\text{div } \mathbf{A} = \partial A_z / \partial z$ was modeled by a comparatively simple linear interpolation between A_z in vacuum and inside the sample. On the other hand the same rapidly varying $A_z(z)$ field will also modify, to some extent, the direct transition contribution $\mathbf{A} \cdot \mathbf{P}_{fi}$, where it enters via $\langle f | A_z(z) p_z | i \rangle$. Due to lack of knowledge, we neglected this contribution. Such neglect was shown to be justified for Al(100) by a jellium calculation^{1,6} but we do not know if this result can be simply transferred to copper.

In conclusion our results clearly demonstrate that any description of $I(\psi)$ based on an analysis considering exclusively the bulk optics is inadequate. We have presented strong evidence that surface electromagnetic fields and the related surface emission must be carefully considered in any interpretation of peak intensities of angle-resolved photoelectron spectra, especially in case of large light incidence angles. Today, where the understanding of photoemission spectra is pushed past traditional limits, reliable data analysis requires to take all possible contributions into account. We hope that our results will also stimulate further theoretical investigation.

ACKNOWLEDGMENTS

Our work was continuously supported by the Deutsche Forschungsgemeinschaft (DFG). We thank G. Meister (Kassel) and W. Pfeiffer (Würzburg) for helpful discussions.

- *Electronic address: agerlach@physik.uni-kassel.de
 †Electronic address: goldmann@physik.uni-kassel.de
 ‡Electronic address: matzdorf@physik.uni-wuerzburg.de
- ¹P. J. Feibelman, *Prog. Surf. Sci.* **12**, 287 (1982).
 - ²*Angle-resolved Photoemission*, edited by S. D. Kevan, *Studies in Surface Science and Catalysis* (Elsevier, Amsterdam, 1992), Vol. 74.
 - ³S. Hüfner, *Photoelectron Spectroscopy—Principles and Applications*, Springer Series in Solid State Science, Vol. 82 (Springer-Verlag, Berlin, 1995).
 - ⁴H. J. Levinson, E. W. Plummer, and P. J. Feibelman, *Phys. Rev. Lett.* **43**, 952 (1979).
 - ⁵H. J. Levinson and E. W. Plummer, *Phys. Rev. B* **24**, 628 (1981).
 - ⁶J. E. Inglesfield and E. W. Plummer, in Ref. 1, Chap. 2, p. 52.
 - ⁷T. Miller, W. E. Mc Mahon, and T. C. Chiang, *Phys. Rev. Lett.* **77**, 1167 (1996).
 - ⁸E. D. Hansen, T. Miller, and T. C. Chiang, *Phys. Rev. Lett.* **78**, 2807 (1997).
 - ⁹M. Born and E. Wolf, *Principles of Optics* (Pergamon, Oxford, 1970).
 - ¹⁰H. Wern and R. Courths, *Surf. Sci.* **152/153**, 196 (1985).
 - ¹¹H. Wern and R. Courths, *Surf. Sci.* **162**, 29 (1985).
 - ¹²A. Gerlach, R. Matzdorf, and A. Goldmann, *Phys. Rev. B* **58**, 10 969 (1998).
 - ¹³R. Matzdorf, A. Gerlach, A. Goldmann, M. Fluchtmann, and J. Braun, *Surf. Sci.* **421**, 167 (1999).
 - ¹⁴R. Matzdorf, A. Gerlach, R. Hennig, G. Lauff, and A. Goldmann, *J. Electron Spectrosc. Relat. Phenom.* **94**, 279 (1998). In contrast to our earlier worked reported in Refs. 12 and 13 we have meanwhile modified the size of the lens system thereby allowing for a larger light spot on the sample without loss of collected photoelectron intensity. This is important especially at grazing light incidence.
 - ¹⁵H. J. Hagemann, W. Gudat, and C. Kunz, *J. Opt. Soc. Am.* **65**, 742 (1975).
 - ¹⁶*Handbook of Optical Constants of Solids*, edited by E. D. Palik (Academic, London, 1998).
 - ¹⁷D. Liese, F. Pforte, T. Michalke, A. Gerlach, G. Meister, and A. Goldmann (unpublished).
 - ¹⁸Ph. Hofmann, K. C. Rose, U. Fernandez, and A. M. Bradshaw, *Phys. Rev. Lett.* **75**, 2039 (1995).
 - ¹⁹B. G. Frederick, J. R. Power, R. J. Cole, C. C. Perry, Q. Chen, S. Hag, Th. Bertrams, N. V. Richardson, and P. Weightman, *Phys. Rev. Lett.* **80**, 4490 (1998).
 - ²⁰J. K. Hansen, J. Bremer, and O. Hunderi, *Surf. Sci.* **418**, L58 (1998).
 - ²¹In a separate optical experiment we verified the validity of the Fresnel's equations and the bulk values ϵ_b on these length scales (Ref. 17). We measured the reflectivity of the used Cu(111) crystal both for *s*- and *p*-polarized light at $\hbar\omega=21.2$ eV. Our results reproduce the real and imaginary part of ϵ_b within 10%.